Wake Turbulence Limits on Paired Approaches to Parallel Runways

David C. Burnham*
Scientific and Engineering Solutions, Inc., Orleans, Massachusetts 02653
James N. Hallock†
John A. Volpe National Transportation Systems Center, Cambridge, Massachusetts 02142
and
George C. Greene‡
Federal Aviation Administration Research and Development Field Office, Hampton, Virginia 23681

Wake turbulence considerations currently restrict the use of parallel runways less than 2500 ft (762 m) apart. However, wake turbulence is not a factor if there are appropriate limits on allowed longitudinal pair spacings and/or allowed crosswinds. The tradeoffs between longitudinal spacing and crosswind, needed to prevent wake encounters, are assessed by modeling and by examining existing wake lateral transport data from O'Hare and Dallas/Ft. Worth airports at distances of 1500–3000 ft (457–914 m) from runway threshold.

I. Introduction

THE safety of aviation operations requires that aircraft not encounter either each other, or the wake turbulence from a larger aircraft. (Dangerous encounters with wake turbulence from an aircraft of the same size are normally avoided by the same separation rules used to prevent midair collisions.) Air traffic control separation standards[1] have been developed to prevent both types of encounter. Current U.S. standards are based on the three aircraft classes listed in Table 1, which are based on maximum certificated gross takeoff weight (MCGTOW). Note that the B-757, although nominally classified as large, has its own separation standards and, therefore, acts much like a fourth class.

A. Parallel Runway Operations

This paper examines parallel runway operations from the wake transport point of view. The air traffic point of view was recently examined[2] in detail; a summary of current parallel runway rules will be presented here. The separation between two parallel runways defines what instrument operations are permitted.

1) Separations of 4300 ft (1311 m) or greater permit simultaneous independent approaches. Such operations are most desirable because neither the controller nor the pilot have to consider what is happening on the other runway.

2) The separation between the runways for simultaneous independent approaches can be reduced to a value as low as 3400 ft (1036 m) for straight-in approaches and 3000 ft (914 m) for angled approaches (Ref. 1, paragraph 5-9-8) if a high-update radar and monitor controller are used to detect aircraft blunders.

3) Runways separated by 2500 ft (762 m) or more can employ simultaneous dependent approaches. Such approaches impose a diagonal separation requirement between aircraft approaching the two runways (Ref. 1, paragraph 5-9-6). Such separations prevent blunders from causing a midair collision. Maintaining the diagonal separation for dependent operations imposes a higher workload on both controllers and pilots than is required for independent operations. The procedure is particularly difficult if the two aircraft are flying at different airspeeds.

4) Finally, runways separated by less than 2500 ft (762 m) (termed close-spaced parallel runways) are treated as a single runway, and simultaneous operations are not permitted. This limit is primarily based on the need to avoid wake turbulence encounters. This rule assumes that wake turbulence from the largest aircraft normally decays to an insignificant level by the time it has traveled 2500 ft (762 m) laterally.

Because the real estate costs of achieving simultaneous, independent approaches is great, many airports have close-spaced parallel runways, which can be used efficiently for simultaneous visual approaches (see next section), but not for simultaneous instrument approaches. When weather conditions deteriorate to the point that instrument approaches are required, such runways suffer a factor of two drop in capacity.

B. Paired Visual Approaches

Visual approaches to close-spaced parallel runways avoid wake turbulence encounters by using a different paradigm than the one used to restrict simultaneous approaches to runways spaced by 2500 ft (762 m) or more. Instead of requiring that wake turbulence never migrate to the parallel runway, the visual approach procedure takes advantage of the time it takes for the wake to travel from one runway to the other. If the paired aircraft have longitudinal separations shorter than the wake travel time, then neither aircraft can encounter the wake of the other. This rationale provides wake turbulence safety for paired, nearly side-by-side, visual approaches to close-spaced parallel runways. Paired visual approaches are routinely used, even for runway spacings as small as 750 ft, (229 m) such as at San Francisco International Airport (SFO).

C. Paired Instrument Approaches

Currently, efforts are underway[2] to extend the wake turbulence safety paradigm of the paired visual approach concept to instrument flight conditions. Note that, in the terminology of Sec. I.A, this procedure is a simultaneous dependent approach. One requirement for validating such procedures is a change in terminology. Current procedures[1] generally define safety in terms of the runway separation, which is the same as aircraft lateral separation for a straight-in approach. A more general definition, based on aircraft lateral separation rather than runway separation, will be needed to deal with paired instrument approaches.

*President. Member AIAA.
†Manager, Aviation Safety Division. Senior Member AIAA.
‡Weather Hazard Project Manager. Associate Fellow AIAA.

Table 1 Wake turbulence classes

Class	MCGTOW, lb
Heavy	>255,000
Large	>41,000; ≤255,000
Small	≤41,000

The primary challenge for paired instrument approaches is to prevent midair collisions. In visual paired approaches, the pilots take responsibility for keeping the aircraft apart, using a "see and seen" philosophy. Such an approach cannot be used under instrument flight conditions. Two methods have been proposed to resolve this question.

In the first, which is possible only with ceilings above a certain level, aircraft are separated laterally by enough distance to meet normal separation criteria, for example, 3000-ft (914-m) lateral separation with high-update radar, until the instrument approach can be converted to a visual approach. The simultaneous offset instrument approach (SOIA) being considered for runways 28L and 28R at SFO adopts this method, which does not require avionics or surveillance technology beyond the current state of the art.

The second method [exploited in the NASA airborne information for lateral spacing program[3] and the Federal Aviation Administration (FAA) paired-approach project[4]] is to use advanced navigation and communications technologies to provide improved situation awareness in the cockpit so that the pilot can fly safely near the other aircraft just as in visual conditions. This method must await the deployment of new technology before it can be implemented.

Of course, both of these methods can be enhanced by current research efforts, for example, the center terminal radar approach control automation system,[5] to develop automated assistance for the air traffic controller.

Whereas the prevention of midair collisions is the most challenging safety requirement of side-by-side instrument approaches, wake turbulence avoidance must also be accomplished before a new procedure can be accepted. Such avoidance can be achieved by various restrictions on the operation, including 1) lead aircraft on downwind runway, trailing aircraft on upwind runway; 2) larger aircraft on downwind runway; 3) larger aircraft trailing; and 4) combined restrictions on crosswind and longitudinal separation. The fourth restriction is examined in this paper.

D. Procedure Implementation

The implementation of side-by-side instrument approaches to close-spaced parallel runways will require the following steps.

1) The necessary research must be done to understand the lateral transport of wake turbulence. This understanding must culminate in a transport model that can be used to simulate the procedure.

2) The safety of the procedure must be validated by FAA Flight Standards (perhaps via simulation using the wake transport model).

3) The appropriate changes must be made to the air traffic control manual[1] to authorize the procedure and instruct controllers how to implement it.

E. Relationship Between Lateral Wake Transport and Crosswind

The operational application of crosswind limits on parallel operations depends on both an understanding of wake transport and the representativeness of the crosswind measurement. NASA's aircraft vortex spacing system (AVOSS)[6] program has investigated both of these issues, particularly as related to single-runway operations. In addition, Hamilton and Proctor[7] have conducted a thorough analysis of how the crosswind affects lateral wake transport using a large-eddy simulation (LES) model. The AVOSS method of handling wind measurement accuracy is used in this paper. Whereas AVOSS was designed to measure wind profiles and other meteorological parameters to predict wake behavior using a complex wake behavior model, this paper adopts both a simple wake transport model and a simple ground-based ambient wind measurement.

II. Crosswind and Longitudinal Spacing Criteria

A. Wake Turbulence Transport Expectations

The expected wake transport depends on proximity to the ground relative to the wingspan of the generating aircraft.

Out of Ground Effect

Out of ground effect (OGE) occurs when the wake is more than one wingspan above the ground. The wake is transported laterally by the ambient crosswind. The wake normally descends because of the mutual interaction of the two wake vortices. Exceptions to descent can occur with atmospheric stratification, thermal activity, or strong crosswind shear. The wake behavior OGE has been studied and modeled, but large statistical databases, for example, 50,000 arrivals, do not exist.

Transition into Ground Effect

As the wake nears the ground, the interaction of the two wake vortices with the ground causes them to separate and stop their normal descent. The wake vortex height reaches a minimum value of about half the initial vortex spacing and then may increase. The behavior of wakes descending into ground effect has been studied and modeled extensively; large statistical databases, for example, more than 50,000 arrivals, are available. This paper analyzes the available landing data relevant to transport between parallel runways.

In Ground Effect

In ground effect (IGE) occurs when the wake is less than half a wingspan above the ground. Wake vortices generated near the ground may not attain their full strength, but also may be at lower altitudes than reached by descending into ground effect. The limited data available on wakes generated IGE suggest that the interaction of the wake with the ground causes rapid lateral motion, but also rapid decay. The wake turbulence tracking system recently installed at SFO has provided statistically significant amounts of data on IGE wakes. The SFO results will be presented later.

On Ground

After an aircraft has landed, much of its weight is carried by the landing gear. However, until the spoilers are deployed, the wings are still generating lift and, hence, generating a wake. Wakes from landing aircraft on the ground have not been studied and are not expected to be a problem. The SFO installation provided relevant data.

B. Lateral Transport is Critical

Wake descent and wake decay play important roles in the wake turbulence safety of single-runway operations, where the longitudinal separations can be 60 s or longer. The longitudinal separations for typical paired approaches are much smaller, perhaps 30 s or less. At SFO, the longitudinal pair separations are kept short so that departures can be launched on the crossing runways between the arriving pairs. For such short separations, the wake has not had much time to descend or decay. In fact, the descent may be less than the vertical variation in flight path. Thus, a robust safety algorithm for side-by-side approaches cannot consider descent or decay, but must be based on lateral transport.

Note that, when the parallel runway thresholds are displaced by more than a few hundred feet, vertical separations can affect the probability of wake encounters. This paper does not examine such configurations.

Using lateral transport alone greatly simplifies the safety analysis. OGE safety can be assessed in terms of the ambient crosswind. IGE safety, where the ground interaction can accelerate the lateral transport, can be assessed by sensors that can track the vortex lateral position (even if the sensors may be unreliable for vortex decay).

If the longitudinal pair separation is small enough, wake turbulence encounters are not possible. For larger longitudinal separations, wake turbulence encounters may become possible when the crosswind is strong enough to move the wake from the leading

aircraft into the path of the following aircraft. Wake turbulence safety then depends on a tradeoff between the maximum allowed longitudinal separation and the maximum allowed crosswind.

C. Effective Crosswind

The development of procedures based on measured or predicted crosswinds must have a safety methodology that can accommodate the way such information can be provided. For example, the AVOSS system provides crosswind values[6] in terms of a mean and standard deviation. The following methodology is proposed.

1) Separation standards are stated in terms of "effective crosswind" limits. The effective crosswind correctly predicts wake lateral transport and can be derived by working backward from observed vortex transport. Although some variation in the effective crosswind could come from possible lateral variations in aircraft positions, such variations can be incorporated into a safety buffer in defining the safety limits on the effective crosswind.

2) The procedure is determined by assessing the probability (based on mean and standard deviation values) that the actual crosswind violates the effective crosswind limits. The safety level is set by how small this probability must be. This analysis must include any variations in crosswind between the measurement location and the wake location.

D. Effective Crosswind Model

Wake turbulence safety can be derived from a model for how the effective crosswind is related to lateral vortex transport. A simple model can be based on the runway spacing D and the effective crosswind v. (Hamilton and Proctor[7] recently presented the results of a complete LES model.) The travel time t for a vortex to reach the parallel runway is roughly

$$t = D/v \qquad (1)$$

The results of Eq. (1) are listed in Table 2 for two airports, SFO ($D = 750$ ft or 229 m) and Boston's Logan (BOS) ($D = 1500$ ft or 457 m), and three effective crosswinds, $v = 20$, 10, and 6 kn. This analysis must be augmented by four important effects that can significantly reduce the travel time.

First, the initial position of the first wake to reach the parallel runway is closer than D. If the vortex-generating aircraft is located on the runway centerline, then the actual distance traveled is reduced by half the vortex spacing b', which is (assuming elliptic wing loading) approximately $(\pi/4)b$, where b is the aircraft wingspan.

Second is IGE, where the interaction of the first wake vortex with the ground will increase its lateral motion by an amount v_i, which may be as large as 4 kn. This interaction does not occur OGE.

Third, safety from a wake vortex encounter requires that the following aircraft keep a distance d [perhaps[8] 100 ft (30 m)] away from a vortex.

Table 2   Tradeoff: maximum effective crosswind v vs maximum longitudinal separation t

		t, s	
v, kn		Eq. (1)	Eq. (2)
		SFO^a	
20	OGE	22	14
20	IGE	——	12
10	OGE	44	28
10	IGE	——	20
6	OGE	74	47
6	IGE	——	28
		BOS^b	
20	OGE	44	36
20	IGE	——	30
10	OGE	89	73
10	IGE	——	52
6	OGE	148	121
6	IGE	——	73

$^a D = 750$ ft. $^b D = 1500$ ft.

Finally, the lateral navigation errors $\pm d_n$ of both aircraft can reduce the distance to be traveled by the first vortex. At the middle marker, d_n may be 50 ft (15 m).

If the worst case of all of these variables are combined, the resulting minimum travel time becomes

$$t = \frac{D - b'/2 - d - 2d_n}{v + v_i} \qquad (2)$$

Table 2 lists the results of Eq. (2) for $b' = 150$ ft (46 m), $d = 100$ ft (30 m), $d_n = 50$ ft (15 m), and $v_i = 4$ kn (only IGE used not OGE). The corrections in Eq. (2) reduce the rough estimates of Eq. (1) by almost a factor of three for the closest runways (SFO) and the smallest crosswind (6 kn).

Because 20 kn can be taken as a reasonable operational upper limit for crosswind, the values in Table 2 suggest what longitudinal separation limits can eliminate any consideration of crosswind. The 30-s IGE value for BOS is possibly a practical value. On the other hand, the 12-s IGE value for SFO is much more restrictive. In fact, the proposed SFO SOIA procedure already incorporates a 10-kn crosswind restriction, which considerably raises the allowed longitudinal spacing (28 s OGE and 20 s IGE).

III.   Available Datasets

Ultimately, the validity of the effective crosswind model must be checked using measurements of lateral wake transport. This paper uses existing wake data for landing aircraft to examine how quickly the wake can travel to a parallel runway: sodar data[9] from O'Hare (ORD) (1976–1997) and windline data from Dallas/Ft. Worth (DFW) (1997–1999). For the two datasets, the crosswind was measured at heights of 50 (15) and 28 ft (8.5 m), respectively. Because this height is typically lower than the wake height, the actual crosswind influencing the wake is normally higher than the measured crosswind, particularly under inversion conditions.

The needed lateral transport distance [see Eq. (2)] for the following analysis is

$$D_T = D - d - 2d_n \qquad (3)$$

which is the distance relative to the runway centerline, not the initial vortex location. The wake data are taken at a given lateral position relative to the runway centerline, not the initial vortex location. The calculated D_T values for SFO and BOS in the vicinity of the middle marker are 550 (169 m) and 1300 ft (396 m), respectively.

A. ORD Vortex Sodar

The ORD vortex sodar installation consisted of two antenna arrays located 1650 (503) and 2150 ft (655 m) from the ends of runways 14R and 32L, respectively. The antenna beam width is approximately 4–6 ft (1.2–1.8 m), and the pulse repetition period is 0.4 s. The accuracy of the vortex arrival at an antenna is typically better than 1 s. Antennas were installed at lateral positions of −1000, −800, −600, −400, −200, 200, and 400 ft (−305, −244, −183, −122, −61, 61, and 122 m). A recent report[9] describes the databases used in the current analysis. The ambient wind was measured approximately 1300 ft (396 m) from the vortex sodars.

The aircraft heights at the ORD sodar locations are approximately 140 ft (43 m). Because the vortex sodar response extends up to 200 ft (61 m) above the ground, vortices passing an antenna can be detected at all possible vortex heights. The aircraft noise decays quickly enough that vortices can be detected within 10 or 15 s after aircraft arrival.

The vortex sodar processing algorithms measure the position and strength of the vortex as it passes each antenna in the array. Although interpolation procedures have been used in prior analyses[10] to give complete wake histories, the analysis of this paper uses the discrete dataset obtained for each antenna.

B. DFW Windline

The DFW windline was located 3225 ft (983 m) from the end of runway 17C and covered lateral positions from −350 to +500 ft (−107 to +152 m) with a pole spacing of 50 ft (15 m) and a pole

height of 28 ft (8.5 m). Each pole includes propeller anemometers that measure the vertical wind and crosswind. The two end poles also measure the headwind. The wind component measurements are averaged for 2 s before being recorded. The windline gives a robust measurement of lateral position for wake vortices that have descended into ground effect and have not decayed significantly. Typical lateral position accuracy is better than 10 ft (3 m). Wakes from over 50,000 arrivals with identified aircraft types were measured by the end of March 1999. Each arrival had at least 60 s of data after the arrival time.

The nominal aircraft height at the windline location is 220 ft (67 m). From this height, the normal descent toward the ground at 2–4 kn can take considerable time. The DFW windline typically detects wakes no sooner than 20 s after aircraft arrival. The windline measurements are fitted to seven parameters: the ambient crosswind and the lateral position, the height and the circulation of the two wake vortices. The resulting database contains measurements every 2 s that a wake vortex is tracked. The DFW windline dataset is used in this paper, first, to analyze vortices that have traveled laterally by 492 ft (150 m) or more. This limit was set just before the end of the array at $+500$ ft ($+152$ m) so that vortex tracking would be valid and was defined in metric units ($+492$ ft $= +150$ m). All measurements with fitted lateral positions greater than $+492$ ft ($+150$ m) were extracted from the database. From these measurements, the data point for each vortex with the lowest vortex age was selected for analysis. (Note that some of the data points could be outliers with anomalous fitted positions. No validity checks were performed because of the large amount of data.) Second, the DFW windline dataset is used to analyze vortex locations at age 30 s. For this analysis, all measurements at 30 s were extracted from the database.

IV.   Travel Times

A.   All Wind Conditions

Figures 1 and 2 present normalized cumulative data on travel times for vortex 1 (downwind vortex, first to arrive at a given location) and vortex 2 (upwind vortex) for lateral positions of 492, 600, 800, and 1000 ft (150, 183, 244, and 305 m). The curves for vortex 1 are plotted with heavier lines and the distances are indicated by the plotting symbol.

Note that vortex 1 arrives more quickly than vortex 2. This result is not surprising because vortex 1 is generated closer to the destination and has an induced transport speed v_i that adds to the ambient crosswind. Vortex 2 is generated farther away and has an induced lateral speed that opposes the crosswind. The ORD data show longer travel times for greater distances, as would be expected.

Table 3 summarizes the results for vortex 1 travel times, which are the limiting factors for paired operations because vortex 1 is the first to reach the path of the following aircraft. Table 3 lists the median travel time (50th percentile) and lower percentiles in the

Table 3   Travel time (seconds) summary for vortex 1

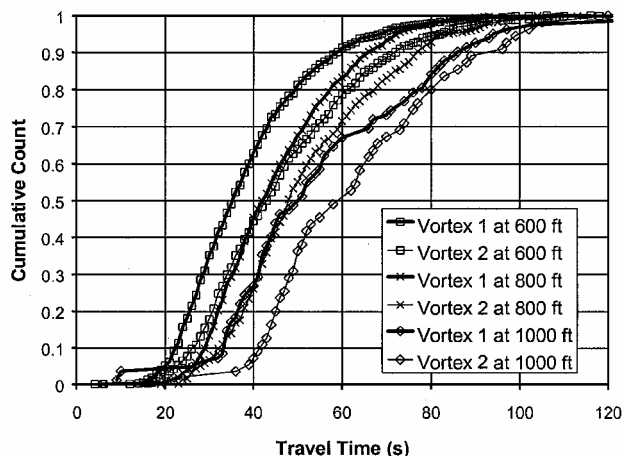| Travel time	DFW 492 ft	ORD 600 ft	ORD 800 ft	ORD 1000 ft
Median	50	35	42	50
25%	39	27	33	39
10%	31	22	29	33
5%	28	20	26	26
2%	24	17	23	——
1%	22	16	21	——

Fig. 2   Normalized cumulative count of travel times to lateral positions of 600, 800, and 1000 ft (183, 244, and 305 m) at ORD.
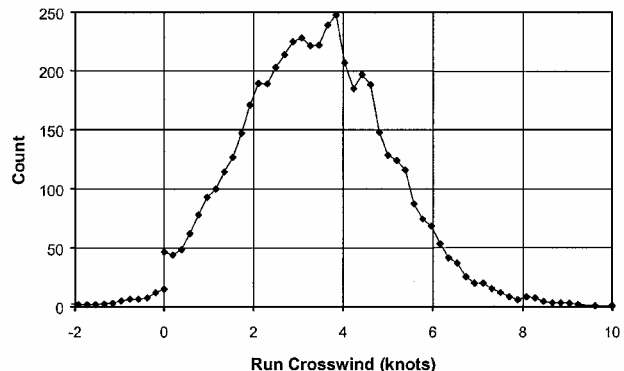

Fig. 3   DFW crosswind distribution for vortex 1 reaching +492 ft (+150 m).

travel time distribution. The travel times are quite different for the datasets from the two airports. The times to reach 492 ft (150 m) at DFW [vortices nominally originate at 220-ft (67-m) altitude] are about the same as the times to reach 1000 ft (305 m) at ORD (vortices nominally originate at 140-ft (43-m) altitude).

B.   Ambient Crosswind Distribution

The time needed for a vortex to reach a given lateral position is determined primarily by the ambient crosswind. Figure 3 shows the distribution of ambient crosswinds [28 ft (8.5 m) height] at DFW (averaged over the 60 s after arrival and taken from the upwind of the windline) for cases when vortex 1 reached $+492$-ft ($+150$-m) lateral position. The bulk of the cases had crosswinds between 0 and $+8$ kn. Only 5 cases had crosswinds of 10 kn or greater.

Figure 4 shows the distribution of ambient crosswinds at ORD for cases when vortex 1 reached -600-ft (-183-m) lateral position. The typical crosswind magnitudes were 4–15 kn, with a maximum magnitude of 25 kn. Thus, the observed crosswinds explain the factor of two faster vortex transport observed at ORD, compared to DFW.

The difference in the observed crosswinds of Figs. 3 and 4 is only partly a difference between the wind characteristics of the
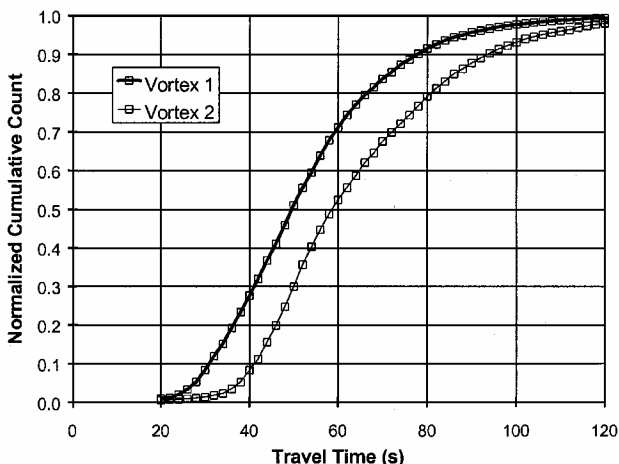

Fig. 1   Normalized cumulative count of travel times to lateral position of 492 ft (150 m) at DFW.
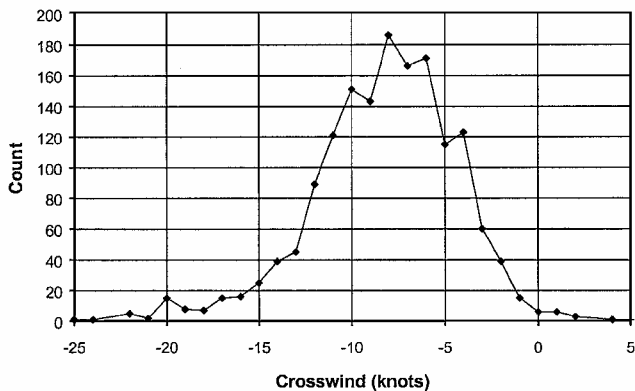
Fig. 4   ORD crosswind distribution for vortex 1 reaching = 600 ft (183 m).
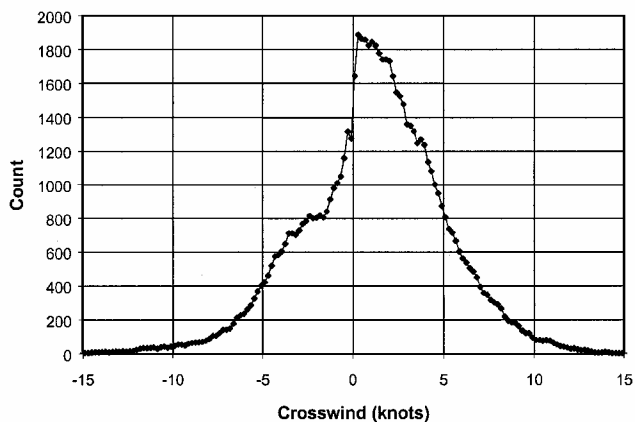

Fig. 5   DFW crosswind distribution for all arrivals.

two airports. It also reflects a difference in the capabilities of the DFW windline and the ORD sodar. Figure 5 shows the crosswind distribution for all of the DFW runs. Whereas the high-crosswind probability is not as great as shown for 600-ft (183-m) transport at ORD in Fig. 4, it is much greater than that for 492-ft (150-m) transport at DFW in Fig. 3. The explanation for the reduced transport probability in strong crosswinds at DFW is that the wake is blown off the end of the windline before it descends to a low enough height to be detected. This effect means that, for short travel times (perhaps less than 40 s), the cumulative count points in Fig. 1 underestimate the actual count.

C.   Ambient Crosswind Limits

Figure 6 compares the distribution of travel times for vortex 1 and 2 at DFW (same data shown in cumulative form in Fig. 1). As mentioned earlier, vortex 1 limits paired approaches. Apart from a jump at 20 s, which may be anomalous (because it is the earliest time for vortex detection in the DFW processing), the vortex 1 count extrapolates to zero at about 20 s.

Figure 7 shows the results of restricting vortex 1 cases on the basis of the ambient crosswind. Selecting crosswinds less than 6 kn affects the distribution. Lower limits cut down the short time side of the travel-time distribution from the left, but leave the higher times unaffected. Note that a crosswind limit below 6 kn should eliminate the cases where the wake leaves the windline before descending low enough to be detected. Thus, windline travel-time distributions for limited crosswinds should be valid. Section V.B will present such an analysis for vortices at age 30 s.

A 6-kn limit has a minimal effect on the travel-time distribution; the extrapolated time to zero count is displaced by roughly 3 s to about 23 s. A limit of 4 kn has a more significant effect; the extrapolated time for zero cases increases to about 28 s. The 2-kn limit further increases the extrapolated zero to well above 30 s, but it also drastically reduces the total number of cases.
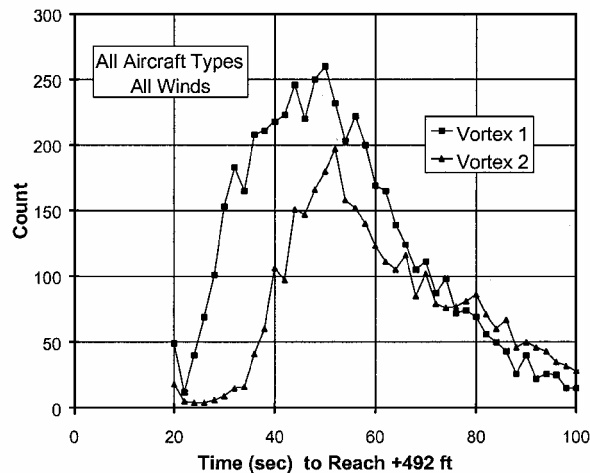

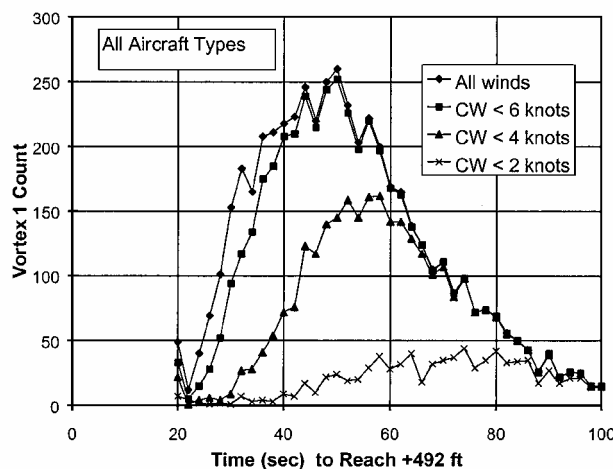Fig. 6   Vortex 1 and 2 travel times to +492 ft (+150 m) at DFW for all aircraft, all winds.

Fig. 7   Vortex 1 travel times at DFW to +492 ft (+150 m) for all aircraft, dependence on run crosswind.
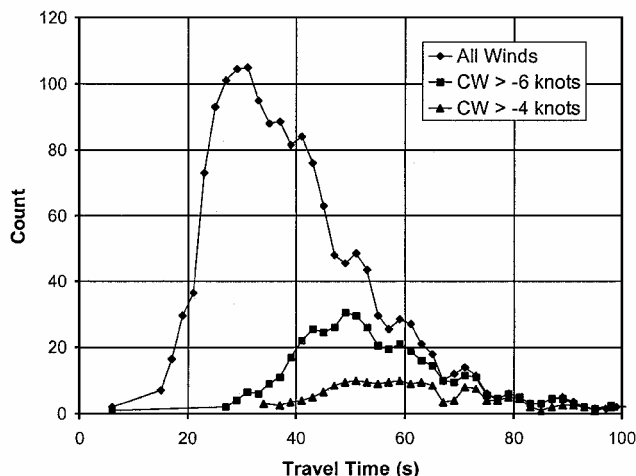

Fig. 8   Vortex 1 travel times at ORD to − 600 ft (− 183 m) for all aircraft, dependence on crosswind.

Figure 8 shows the effect of crosswind limits on the ORD travel-time distribution for reaching −600 ft (−183 m). The 6-kn limit has a much greater impact on the ORD data than the DFW data in Fig. 7 because the DFW travel-time data already exclude most crosswinds above 6 kn. Note, however, that the 6- and 4-kn limits in Figs. 7 and 8 give comparable travel-time distributions for the two airports. The much larger number of cases for the DFW dataset (76,000 vs 8,000 for ORD) gives more definitive travel-time distributions.

Table 4 Wake vortices reaching +492-ft lateral position in ≤30 s vs aircraft type in order of descending size

Aircraft type	Total cases	Cases at +492 ft	
		Vortex 1	Vortex 2
MD11	325	9	0
DC10	470	15	0
L1011	409	10	0
B767	1,619	24	0
B757	4,482	48	1
B727	6,961	51	7
B737	1,422	5	1
MD88	2,674	25	1
MD80	22,277	193	18
DC9	1,928	2	3
FK100	1,780	9	3
SF340	5,737	14	6
AT72	1,735	8	4
EMB120	2,687	10	2

Table 5 Data points for largest aircraft

Points	Vortex 1	Vortex 2
1	41	1
2	64	2
3	25	1
4	14	——
5	2	1
6	——	2
7	2	——
8	1	1
9	1	——
10	2	——
12	1	——
14	1	——
17	1	——
21	1	——
30	1	——

Fig. 9 B-757 vortex transport speed–crosswind: top vortex 1 and bottom vortex 2.

D. Short DFW Travel Times

Table 4 lists the vortices reaching +492-ft (+150-m) lateral position in 30 s or less. The vortices are disaggregated by aircraft type; the total number of arrivals is also listed for each aircraft type to provide normalization for the short travel cases.
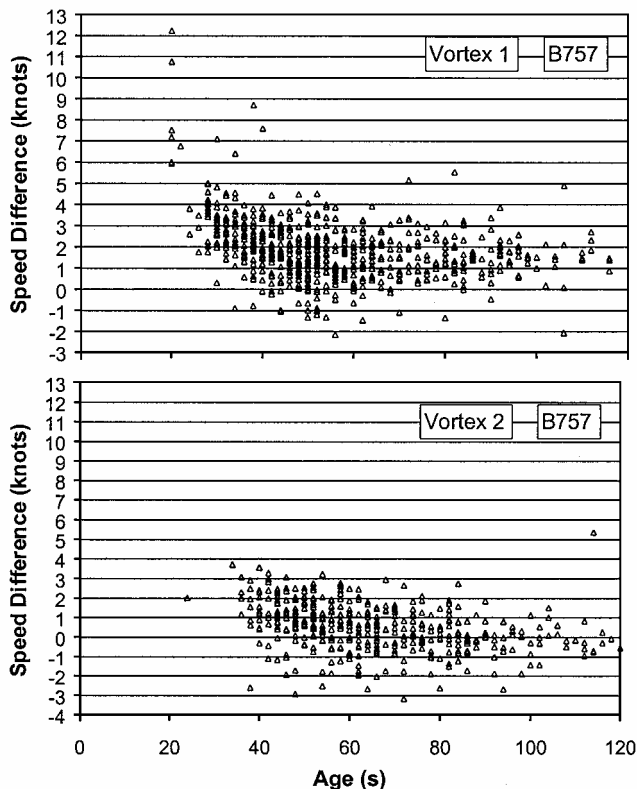
For the purposes of wake turbulence safety, the behavior of wakes from the largest aircraft is most significant. The fraction of vortices reaching +492 ft (+150 m) is also greater for the largest aircraft in Table 4. Therefore, consider the 165 cases for the following aircraft types: MD11, DC10, L1011, B767, B757, and B727. Table 5 examines how many times each vortex was detected beyond 492-ft lateral position. A greater number of points gives more confidence that the case is valid. The single-point cases are less than one-third of the total. On the other hand, cases with more than two points are also less than one-third of the total. Because +492 ft (+150 m) is near the end of the windline at 500 ft (152 m) and vortices reaching +492 ft (+150 m) in a short time are moving fast, it is not surprising that the typical number of vortex detections beyond +492 ft (+150 m) is small.

V. Effective Crosswind Analysis

Section II.C defined an effective crosswind that takes into account all wake transport effects, but excludes any errors in measuring the crosswind. Unfortunately, the analysis of Sec. IV includes both effects. The goal of this section is to distinguish the wake transport effects from the crosswind measurement effects, so that the division of Sec. II.C can be implemented and the lateral transport model of Sec. II.D can be validated.

A. Transport Speed Versus Crosswind

This section examines the relationship between vortex transport speed and the ambient crosswind. The initial lateral positions of the two wake vortices are assumed to be

$$y_i = \pm \pi b/8 \qquad (4)$$

where b is the wingspan and the plus sign pertains to vortex 1 and the minus sign to vortex 2. The nominal vortex transport speed v to reach lateral position y is, therefore, given by

$$v = (y - y_i)/t \qquad (5)$$

where t is the travel time.

Figure 9 compares the calculated B-757 vortex transport speeds with the ambient crosswind for vortex 1 (top) and vortex 2 (bottom) as a function of travel time. For short travel times the data are biased toward higher vortex transport speeds because fast transport is required to reach +492 ft (+150 m) in a short time and the ambient wind has considerable variance with respect to the vortex transport because it is measured on the other end of the windline. This bias is most evident in the top plot of Fig. 9.

Crosswind shear also contributes to the bias because the crosswind is measured at 28 ft (8.5 m) height, whereas the fast-moving vortices spend most of their travel time at much greater heights where the crosswind is normally also greater. Older vortices spend more of their travel time closer to the ground. For vortex 1, the mean transport–crosswind difference is about 3.0 kn at 30-s travel time, but drops to a value of about 2.6 kn at 40-s travel time and reaches an asymptotic value of about 1.6 kn at 60-s travel time. For vortex 2, the mean transport-crosswind difference is about 1.6 kn at 40-s travel time, but drops to an asymptotic value of about 0.4 kn at 80-s travel time. The transport speed difference between vortex 1 and 2 is roughly 1.0–1.2 kn, which is significantly less than the normal ground effect separation rate, which would be roughly 6 kn. The reduction in transport speed difference is due to two effects: 1) the large amount of time spent OGE and 2) vortex decay.

Because of the bias introduced by selecting cases with vortex detection at a specific location, the data in Fig. 9 cannot readily be separated into vortex transport effects and wind measurement effects. (The same problem was noted in Ref. 9.)

B. Analysis at 30-Second Separation

The biases of selecting vortices reaching a given lateral position can be avoided by looking at vortices of a given age. This section examines DFW vortex characteristics at age 30 s, which is a possible usable limit on longitudinal separation of arrival pairs.

Figure 10 shows the distribution of measured vortex locations at 30 s. The minimum crosswind vortex starts at negative lateral positions (port vortex) and the maximum crosswind vortex starts at positive lateral positions (starboard vortex). At 30 s, the two vortices show a significant probability of reaching only the end of the line on their original side of the runway centerline; note the sharp drop in cases at the ends of the anemometer array [-350 ft (-107 m) for minimum vortex and $+500$ ft ($+152$ m) for maximum vortex]. These sharp breaks suggest that many vortices are not detected because their locations are outside the array. The bias toward positive crosswinds (Fig. 5) generally drifts the position distribution for both vortices to the right in Fig. 9.

One way of avoiding the biases of restricting vortex locations is to choose a range of measured crosswinds that result in few vortices reaching the ends of the anemometer array. Figure 11 shows the position distribution for measured crosswinds between 0 and 4 kn, which encompasses about 40% of the arrival cases (Fig. 5). The selection of this range of crosswinds has successfully eliminated the sharp breaks at the ends of the anemometer array. Thus, virtually all of the vortices have been detected, and no selection biases should be present.

This unbiased dataset can be used to examine the relationship between the effective crosswind and the measured crosswind. The
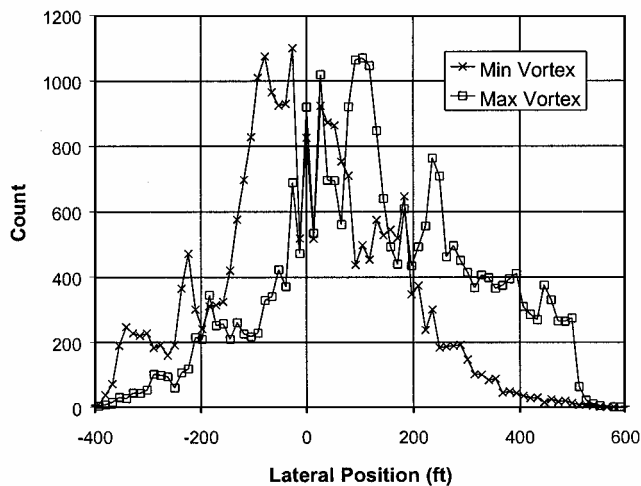

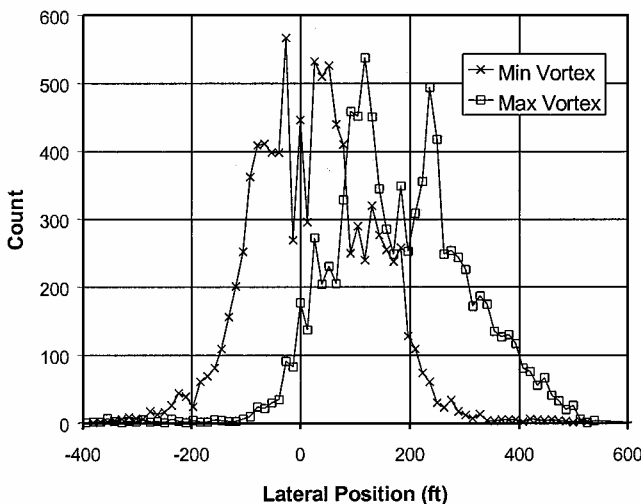**Fig. 10   DFW vortex position distribution at 30 s.**

Fig. 11   DFW vortex position distribution at 30 s for measured crosswind: 0–4 kn.

Table 6   Statistics of crosswind difference (knots)

Aircraft	V	Count	Mean[a]	Stdev[b]	Skew[c]	Kurt[d]
MD80	0	3358	−0.3	1.6	−0.4	2.9
——	1	3157	1.0	1.9	−0.2	3.4
B727	0	1169	−0.4	1.6	−0.1	2.5
——	1	1077	1.0	1.9	−0.9	7.4
B757	0	857	−0.3	1.5	−0.4	1.3
——	1	851	0.9	1.7	0.2	2.6
B767	0	362	−0.2	1.5	−0.2	1.2
——	1	351	0.8	1.6	−0.1	0.5
L1011	0	98	−0.3	1.5	0.4	1.0
——	1	98	1.0	1.5	0.6	0.4
DC10	0	81	0.0	1.7	0.6	2.4
——	1	78	1.1	1.5	0.5	0.1

[a] Average difference.
[b] Standard deviation, width of the distribution.
[c] Asymmetry of the distribution: negative skew means a negative tail to the distribution.
[d] Kurtosis, positive kurtosis means that the distribution has higher tails than a normal distribution.

Table 7   Crosswind shear, induced vortex motion

Aircraft	Shear, kn	Induced, kn
MD80	0.7	0.7
B727	0.6	0.7
B757	0.6	0.6
B767	0.6	0.6
L1011	0.6	0.7
DC10	1.1	0.7

analysis makes use of Eqs. (4) and (5) to calculate the effective transport speed v for each vortex. The initial position is assumed to be given by Eq. (4), and the measured lateral position at time $t = 30$ s is taken as y in Eq. (5). The crosswind difference is then taken as the transport speed minus the measured crosswind during the first 60 s of the run. The results are treated statistically rather than graphically and are presented in Table 6 for six aircraft types. The two vortices are designated by $V = 0$ for the minimum crosswind vortex (port vortex) and $V = 1$ for the maximum crosswind vortex (starboard vortex). Table 6 lists the number of vortices and four statistical parameters for the crosswind difference.

The mean difference between the transport speed and measured crosswind represents two effects: First is the difference between the crosswind experienced by the vortex and the measured wind, that is, the crosswind shear. The vortex is typically higher than the 28-ft (8.5-m) anemometer height and, hence, has a somewhat stronger crosswind. This difference is the same for both vortices and can be calculated as the average of the mean difference for the two vortices. The second effect is the vortex motion induced by the ground, which has the opposite sign for the two vortices and can be calculated as half the difference between the crosswind differences for the two vortices.

The calculated crosswind shear and induced motion values are presented in Table 7. Apart from the DC10 shear value, the results in Table 7 are very consistent. (Note that the DC10 had the fewest cases.) The induced motion values are smaller than usually stated for ground effect, but are not surprising because the vortices spent much of their 30-s history away from the ground.

The standard deviation values in Table 6 range from 1.5 to 1.9 kn. The small size of these variances is likely due to the close temporal and spatial proximity to vortices. Section II.C distinguished between the effective crosswind, which details wake effects, and wind measurement.

1) The vortex-induced motions in Table 7 must be assigned to the effective crosswind. Note that the values are much smaller than the 4 kn assumed in Table 2. Thus, the results of Table 2 would be conservative for the windline location at DFW.

2) The shear in Table 7 and the standard deviation (also skew and kurtosis) of Table 6 must be assigned to wind measurement errors. Because the shear is typically proportional to the crosswind and a

maximum crosswind of 4 kn was used in the analysis of Table 6, it is likely that significantly larger shears would be observed for stronger crosswinds. Likewise, for shorter times, a vortex would be typically farther from the ground and would experience a larger difference from the 28-ft (8.5-m) wind measurement. In an operational situation, crosswind measurements may need to cover the entire flight region where the aircraft pair have lateral separations comparable to the runway spacing.

VI. Recommendations

The major limitation of the analysis of this paper was the lack of sufficient lateral coverage of the windline data, which turned out to be more useful than the sodar data for the analysis because of its continuous tracking of the wakes. Extending the windline coverage would provide the data needed to validate the effective crosswind model for all operational crosswinds, not just the 0–4 kn band.

A substantial windline dataset on vortex transport between parallel runways has been collected[11] at the Frankfurt, Germany, Airport. The analysis of this data has begun; it may provide useful transport statistics over greater lateral distances than available from U.S. data.

A complete understanding of wake turbulence transport for paired approaches must cover the entire approach path where the lateral spacing is close. The least studied region is ground effect where little data are available. The recently installed SFO windline should provide the missing data.

VII. Conclusions

This paper proposed a method for developing wake turbulence safety criteria for side-by-side instrument approaches to close-spaced parallel runways. The safety criteria are based on the effective crosswind that defines lateral wake transport. Differences between the effective crosswind and the measured crosswind represent wind measurement errors. A model is proposed for defining the effective crosswind.

Wake lateral transport data from two airports (ORD and DFW) were examined. To prevent wake encounters, the following relationships between crosswind and longitudinal pair spacing can be supported.

1) The ORD data suggest (Fig. 3) that runways separated by no more than 1000 ft (305 m) will permit longitudinal pair separation of not much greater than 20 s if no crosswind criteria are applied.

2) For runways separated by about 600 ft (183 m), limiting crosswinds from leader toward follower to 6 kn will support longitudinal pair separation from 23 (DFW) to 25 (ORD) s. Reducing the allowed crosswinds to 4 kn increases the allowed pair separation to 28 (DFW) s.

Selecting wakes that have traveled a certain distance leads to biases that prevent a clear division between wake transport and wind measurement errors. These biases can be eliminated by examining wakes at a certain age, for example, 30 s, and selecting crosswind criteria that prevent wake vortices from being lost off the ends of the measurement array. The DFW windline data provided consistent values for ground-induced vortex motion and wind measurement biases and variance. The DFW values for ground-induced motion are well within the limits of the proposed effective crosswind model.

Note that the development of safety criteria for instrument side-by-side approaches should also improve the safety of visual side-by-side approaches.

References

[1] "Air Traffic Control," Federal Aviation Administration, FAA Order 7110.65M, Feb. 2000.

[2] Burnham, D. C., Hallock, J. N., and Greene, G. C., "Increasing Airport Capacity with Modified IFR Approach Procedures for Close-Spaced Parallel Runways," *Air Traffic Control Quarterly*, Vol. 9, No. 1, 2001, pp. 45–58.

[3] Waller, M. C., Doyle, T. M., and McGee, F. G., "An Analysis of the Role of ATC in the AILS Concept," NASA/TM-2000-210091, April 2000.

[4] Hammer, J., "Case Study of Paired Approach Procedure to Closely Spaced Parallel Runways," *Air Traffic Control Quarterly*, Vol. 8, No. 3, 2000, pp. 223–252.

[5] Denery, D. G., Erzberger, H., Davis, T. J., Green, S. M., and McNally, B. D., "Challenges of Air Traffic Management Research: Analysis, Simulations, and Field Test," AIAA Paper 97-3832, Aug. 1997.

[6] Hinton, D. A., "An Aircraft Vortex Spacing System (AVOSS) for Dynamical Wake Vortex Spacing Criteria," *The Characterization and Modification of Wakes from Lifting Vehicles in Fluids*, CP-584, AGARD, Nov. 1996, pp. 23–(1–12).

[7] Hamilton, D. W., and Proctor, F., "Wake Vortex Transport in Proximity to the Ground," 19th Digital Avionics Systems Conf., Paper 3.E.5, AIAA and IEEE, Philadelphia, PA, Oct. 2000.

[8] McWilliams, I. G., "Hazard Extent About Aircraft Trailing Wake Vortices: Analytic Approach," *Proceedings of the Aircraft Wake Vortices Conference*, Federal Aviation Administration, Cambridge, MA, June 1977, pp. 23–30.

[9] Burnham, D. C., and Hallock, J. N., "Wind Effects on the Lateral Motion of Wake Vortices," Volpe National Transportation Systems Center, DOT/FAA/AAR-99-88, Cambridge, MA, Nov. 1999.

[10] Hallock, J. N., and Burnham, D. C., "Chicago Monostatic Acoustic Vortex Sensing System: Vol. II: Decay of B-707 and DC-8 Vortices," Transportation Systems Center, DOT/FAA/RD-79-103, II, Cambridge, MA, Sept. 1981.

[11] Hallock, J. N., Burnham, D. C., Jenkins, J., Konopka, J., and Rudolph, R., "Wake Vortex Tracking Using Frankfurt Windline," European Geophysical Society, 25th General Assembly, Paper OA24-020, April 2000.